

# Analysis and Evaluation of Handwriting in Patients with Parkinson's Disease Using kinematic, Geometrical, and Non-linear Features

C. D. Rios-Urrego<sup>1</sup>, J. C. Vásquez-Correa<sup>1,2\*</sup>, J. F. Vargas-Bonilla<sup>1</sup>, E. Nöth<sup>2</sup>, F. Lopera<sup>3</sup>, and J. R. Orozco-Arroyave<sup>1,2\*</sup>

<sup>1</sup>Faculty of Engineering, University of Antioquia UdeA, Medellín, Colombia.

<sup>2</sup>Pattern Recognition Lab, Friedrich-Alexander-Universität Erlangen-Nürnberg, Germany.

<sup>3</sup>Neuroscience Research Group, Faculty of Medicine, University of Antioquia UdeA, Medellín, Colombia.

## Abstract

**Background and objectives:** Parkinson's disease is a neurological disorder that affects the motor system producing lack of coordination, resting tremor, and rigidity. Impairments in handwriting are among the main symptoms of the disease. Handwriting analysis can help in supporting the diagnosis and in monitoring the progress of the disease. This paper aims to evaluate the importance of different groups of features to model handwriting deficits that appear due to Parkinson's disease; and how those features are able to discriminate between Parkinson's disease patients and healthy subjects.

**Methods:** Features based on kinematic, geometrical and non-linear dynamics analyses were evaluated to classify Parkinson's disease and healthy subjects. Classifiers based on K-nearest neighbors, support vector machines, and random forest were considered.

**Results:** Accuracies of up to 93.1% were obtained in the classification of patients and healthy control subjects. A relevance analysis of the features indicated that those related to speed, acceleration, and pressure are the most discriminant. The automatic classification of patients in different stages of the disease shows  $\kappa$  indexes between 0.36 and 0.44. Accuracies of up to 83.3% were obtained in a different dataset used only for validation purposes.

**Conclusions:** The results confirmed the negative impact of aging in the classification process when we considered different groups of healthy subjects. In addition, the results reported with the separate validation set comprise a step towards the development of automated tools to support the diagnosis process in clinical practice.

**Keywords:** Parkinson's disease, Handwriting, kinematic features, Geometrical features, Non-linear dynamics

## 1. Introduction

Parkinson's disease (PD) is a neuro-degenerative disorder, which produces motor and non-motor symptoms in the patients. Examples of motor impairments include resting tremor, bradykinesia, rigidity, micrographia, hypomimia, and others [1]. While examples of non-motor impairments include depression, sleep disorders, dementia, and others [2]. These symptoms appear as consequence of the progressive loss of dopaminergic neurons in the mid-brain [1]. Handwriting is one of the most impaired motor activities in PD patients. The most common symptoms in handwriting of PD patients include micrographia, which is related to the reduction of the size in handwriting, and dysgraphia, which is related to difficulties performing the controlled fine motor movements required to write [3]. The progression of motor symptoms is currently evaluated with the third section of the Movement Disorder Society – Unified Parkinson's Disease Rating Scale (MDS-UPDRS-III) [4], which is administered by neurologist experts. The scale contains several aspects to evalu-

ate motor skills of the patients, including those directly or indirectly related with handwriting like finger tapping, hand tremor, hand rigidity, and others. The diagnosis process of PD is expensive and time-consuming for patients, caregivers, and the health system [5, 6, 7]. Automatic handwriting analysis could help to support the process to diagnose and monitor the neurological state of the patients.

There is interest in the research community to automatically assess the handwriting of PD patients. Most of the studies consider data from on-line handwriting, which are captured from digitizer tablets, and contain information related to the dynamics of the handwriting process while the patient is putting the pen on the tablet (i.e., on-surface). Some of the features that are typically extracted from the on-surface dynamics include the pressure of the pen, and the azimuth and altitude angles. There are also tablets that allow to capture information of the in-air movement (i.e., before and/or after the patient to put the pen on the tablet's surface). The classical way of addressing the analysis of on-line handwriting is based on on-surface features. For instance in [8] the authors proposed features related to the power spectral density of the speed stroke in the handwriting of 17 healthy control (HC) subjects and 13 PD patients. The authors classified PD patients vs. HC subjects using a neural network and reported an accuracy of up to 86.2%. In [9] the au-

\*corresponding author J. C. Vásquez-Correa

e-mail: juan.vasquez@fau.de

Address: Friedrich-Alexander-Universität Erlangen-Nürnberg (FAU) Lehrstuhl für Informatik 5 (Mustererkennung) Martensstr. 3, Of 10.158, 91058 Erlangen Germany

thors extracted kinematic features from the handwriting of 20 HC subjects and 20 PD patients who wrote their addresses and full names. The authors computed features related to the average time on the tablet’s surface, the average in-air time of the pen, the speed of the trajectory, and the average pressure of the pen. The authors reported accuracies of up to 97% in the classification of PD patients vs. HC subjects. In [10] the authors evaluated the in-air movement during the handwriting process of 37 PD patients and 38 HC subjects who wrote the Czech sentence: *Tramvaj dnes uz nepo-jede* (the train will not go today). The authors extracted several kinematic features including the average in-air time of the pen, and the average on-surface time. The authors performed the classification of PD patients and HC subjects using a support vector machine (SVM) with a Gaussian kernel, and reported accuracies around 86% when the features based on pressure, kinematic, in-air time, and on-surface time are combined. In [11] the authors analyzed different handwriting tasks performed by the same set of patients considered in [10]. The set of tasks included the Archimedean spiral, the repetition of the graphemes *l* and *le*, simple orthographic isolated words, and the Czech sentence: *Tramvaj dnes uz nepo-jede*. The authors extracted kinematic and pressure-based features to classify PD patients and HC subjects. Three different classification methods were considered: SVM, K-nearest neighbors (KNN), and Adaboost. Accuracies of up to 76.5% were reported with the combination of kinematic and pressure-based features. In [12] the authors applied the Generalized Canonical Correlation Analysis (GCCA) to classify PD patients and HC subjects, and to predict the neurological state of the patients using information from handwriting, speech, and gait. Handwriting analyses were based on kinematic features extracted from the vertical and horizontal axes, and the pressure of the pen. The authors concluded that the combination of speech, handwriting, and gait using the GCCA approach improves the accuracy in the classification and the prediction of the neurological state.

Other neurological disorders have also been studied using online handwriting. In [13] the authors proposed non-linear dynamics (NLD) features to evaluate the handwriting of 10 HC subjects and 25 patients with essential tremor. Several NLD features such as the fractal dimension and Shannon entropy were extracted from the Archimedean spiral. The NLD features were combined with standard kinematic measures related to the speed and pressure of the pen. The authors reported accuracies of up to 85% classifying the patients vs. HC subjects.

Recent deep learning approaches have also been used to classify handwriting of PD and HC subjects. In [14] the authors modeled the handwriting dynamics of 18 HC and 74 PD subjects using a smart-pen with several sensors. The participants performed several tasks including the drawing of circles and Archimedean spirals. The authors proposed a model based on convolutional neural networks (CNNs). The signals from the smart-pen were transformed into images by concatenating and reshaping the time-series. Several CNN configurations were considered for each task, and a majority voting scheme was implemented to make the final decision. Accuracies up to 95% were reported by the authors. In [15] the authors considered a

model called deep echo state network to classify 67 PD patients and 15 HC subjects who drew Archimedean spirals on a tablet. The deep learning model was based on recurrent neural networks (RNNs), which process the time-series of horizontal and vertical movements, the grip angle, and the pressure of the pen. The authors reported accuracies of up to 88.3% with the proposed model. Recently, in [16] researchers from our research Lab considered a deep learning model based on CNNs to classify PD patients and HC subjects using multimodal information from speech, handwriting, and gait. The handwriting analysis was based on the transition when the patients have the pen in the air and put it on the tablets surface. The trajectories from the pen and the pressure of the pen were modeled with a CNN. The authors reported accuracies of up to 97.6% when information from speech, handwriting, and gait is combined; however, the accuracy obtained considering only the handwriting analysis was around 66.5%.

According to the reviewed literature, most of the studies considered kinematic features to evaluate handwriting impairments of patients with neurodegenerative disorders. There are some recent studies that consider deep learning methods to assess the handwriting deficits of PD patients. Other kinds of features including geometrical, spectral, and NLD based have not been extensively studied to support the diagnosis and monitoring of the patients. The analysis of these aspects will be the main outcomes of the current study.

### 1.1. Research objectives of this study

This paper evaluates the performance of three different feature sets (kinematic, geometrical, and NLD) to model handwriting impairments of PD patients. The method aims to provide suitable insights about the relevance of different features to discriminate between PD patients and HC subjects. The proposed approach is evaluated in realistic conditions, i.e., with a different sets of patients and healthy subjects that never participated in the training process. Finally, the study aims to evaluate the suitability of the proposed approach to automatically classify patients in different stages of the disease.

## 2. Data Acquisition and Participants

The data were collected with a Wacom Cintiq 13 HD tablet, with visual feedback to the patients and using a sampling frequency of 180 Hz. The tablet captures six different signals: horizontal position ( $x(t)$ ), vertical position ( $y(t)$ ), azimuth angle, altitude angle, distance to the tablet surface ( $z(t)$ ), and pressure of the pen. For this study the participants draw an Archimedean spiral following a predefined template (Figure 1), which was displayed on the tablet. Participants were requested to draw the spiral between the lines of the template and avoiding to cross them. Additionally, the participants wrote the sentence “*El abecedario es a, b, c, ..., z*” which in English is: “*The alphabet is a, b, c, ..., z*”.

With the aim to show real cases of how people with different age and health condition draw, Figures 2 and 3 include examples of drawings obtained from three different participants:

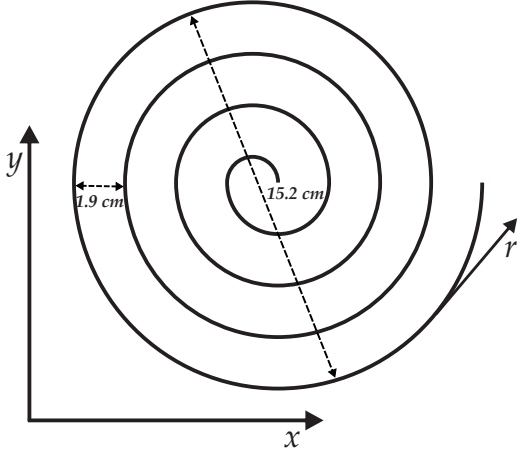


Figure 1: Template of the Archimedean spiral.

23 years old subject (left), 65 years old subject (middle), and 73 years old PD patient with a MDS-UPDRS-III score of 64 (right).

### 2.1. Subjects

Four groups of participants are considered in this study: patients with PD; elderly HC subjects; young HC subjects; and an additional set of 12 participants, which is considered to validate the generalization capability of the models. Details of each group are provided below.

#### *PD patients:*

This group is formed with 39 patients (26 female) with ages between 29 and 81 years (mean = 59.08; SD = 11.17). All of them were evaluated by a neurologist expert according to the MDS-UPDRS-III scale [4]. The scores of such evaluations ranged between 8 and 106 (mean = 35.72; SD = 23.25). This group of patients was recruited in the Foundation for Parkinson’s patients in Medellín, Colombia. The patients were evaluated during the “ON” phase of medication, i.e., no more than three hours after the intake.

#### *Elderly HC subjects (eHC):*

This group includes 39 healthy subjects (18 female) with ages between 29 and 85 years (mean = 61.85; SD = 13.89). None of the participants in this group had symptoms of neurological or movement disorders. The PD and eHC groups are matched for age ( $t(0.99) = -1.19, p = 0.12$ ).

#### *Young HC subjects (yHC):*

A total of 40 healthy participants (16 female) are included in this group. The age ranges from 20 to 42 years (mean = 24.43; SD = 4.08). Most of the participants of this set are students who wanted to participate in the study. None of them exhibited or manifested symptoms of neurological or movement disorders.

Table 1 includes demographic and clinical data of the subjects included in the aforementioned three groups. Figure 4 shows the age distribution of the three groups of subjects.

#### *Additional validation set:*

This group of subjects was considered to validate the generalization capability of the model proposed in this paper. The

group includes 6 PD patients and 6 HC subjects, there are 3 female in each group, and the ages range from 54 to 83 (mean = 68.33; SD = 10.19) and from 45 to 57 (mean = 53; SD = 4.69), respectively. Demographic and clinical data, including the MDS-UPDRS-III score of each patient in this additional validation set, are included in Table 2.

## 3. Methods

The methodology addressed in this work consists of three main stages: feature extraction, dimensionality reduction, and automatic classification. This methodology is summarized in Figure 5. Details of each stage are presented in the following subsections.

### 3.1. Feature Extraction

Three different feature sets are extracted from the signals: features based on kinematic analysis, novel features based on the geometrical and spectral analyses of the Archimedean spiral, and NLD features.

#### 3.1.1. kinematic features:

A total of eight features are extracted: (1) absolute/real trajectory of the Archimedean spiral  $r(t)$ , computed as  $r(t) = \sqrt{x^2(t) + y^2(t)}$ , where  $x(t)$  and  $y(t)$  are the horizontal and vertical positions, respectively; (2) speed of the trajectory; (3) acceleration of the trajectory; (4) pressure of the pen; (5) first derivative of the pressure; (6) second derivative of the pressure; (7) distance from the tablet’s surface to the pen ( $z(t)$ ); and (8) first derivative of  $z(t)$ . Six functionals are computed for each feature: mean, standard deviation, maximum value, minimum value, skewness, and kurtosis, forming a 48-dimensional feature vector per drawing.

#### 3.1.2. Geometrical and spectral features

A novel feature set with geometrical and spectral measures of the Archimedean spiral is introduced. To create the feature set the spiral’s trajectory is modeled as the amplitude-modulated signal  $\widehat{r}(t)$  defined in Equation 1.

$$\widehat{r}(t) = (a_3t^3 + a_2t^2 + a_1t + a_0) \cdot \sin(2\pi ft) \quad (1)$$

The real trajectory  $r(t)$  is modeled as a sinusoidal signal with increasing amplitude and frequency  $f$ . The amplitude values are given by a third-order polynomial which coefficients ( $a_i$ ) are estimated using a polynomial regression with the maximum peaks of the original trajectory. A third-order polynomial is chosen because it avoids an oscillatory behavior across the samples. Additionally, the third order guarantees a smooth first derivative and a continuous second derivative across the trajectory [17]. The frequency  $f$  is obtained as the fundamental frequency of the trajectory using the Fourier transform. The model of the trajectory is depicted in Figure 6 where the real and the modeled trajectories can be compared. Note that the trajectory for the PD patient is more irregular than those observed for the two HC subjects. Twelve features are extracted from the modeled trajectory: mean square error (MSE) between the real and

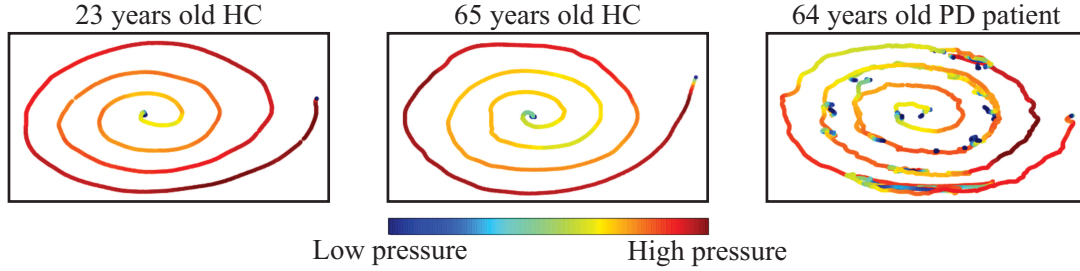


Figure 2: Archimedean spiral drawn by three participants.

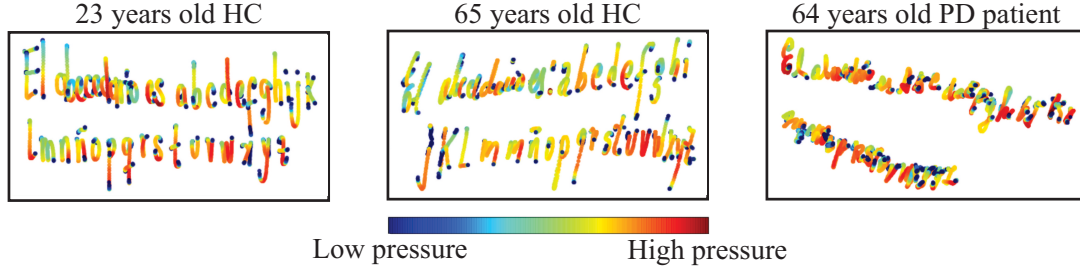


Figure 3: Sentence written by a yHC (left), an eHC (middle), and a PD patient (right). The sentence is: *El abecedario es a b c ... z.*

Table 1: Demographic and clinical information of the participants. **PD**: Parkinson's disease, **eHC**: elderly healthy controls, **yHC**: young healthy controls,  $\mu$ : average,  $\sigma$ : standard deviation.

	<b>PD patients</b>		<b>eHC</b>		<b>yHC</b>	
	<b>Male</b>	<b>Female</b>	<b>Male</b>	<b>Female</b>	<b>Male</b>	<b>Female</b>
Number of subjects	13	26	21	18	24	16
Age ( $\mu \pm \sigma$ )	$62.8 \pm 10.2$	$57.7 \pm 11.4$	$67.4 \pm 12.8$	$60.5 \pm 8.0$	$25.3 \pm 4.5$	$23.1 \pm 3.0$
Age range	41 – 81	25 – 71	49 – 84	50 – 74	21 – 42	20 – 32
Time post diagnose (years) ( $\mu \pm \sigma$ )	$8.4 \pm 4.5$	$13.4 \pm 12.7$				
MDS-UPDRS-III ( $\mu \pm \sigma$ )	$34.6 \pm 22.1$	$36.3 \pm 24.2$				
Range of MDS-UPDRS-III	8 – 82	9 – 106				

Table 2: Demographic and clinical information of the participants in the additional validation dataset. **PD**: Parkinson's disease, **HC**: healthy controls, **t**: time post diagnose [years], **UPDRS-III**: MDS-UPDRS-III.

<b>HC</b>			<b>PD</b>				
<b>Gender</b>	<b>Age</b>		<b>Gender</b>	<b>Age</b>	<b>t</b>	<b>UPDRS-III</b>	
HC 1	M	57	PD 1	F	65	8	24
HC 2	F	45	PD 2	F	69	5	26
HC 3	F	50	PD 3	M	63	6	36
HC 4	F	57	PD 4	M	76	14	69
HC 5	M	54	PD 5	M	54	5	43
HC 6	M	55	PD 6	F	83	6	34

modeled trajectories, the coefficients of the third order polynomial used for the model ( $a_i, i \in \{0, 1, 2, 3\}$ ), amplitude of the first five spectral components of the trajectory, the slope of the line that links the peaks of the first and third spectral components of the trajectory, and the slope of the line that links the amplitudes of the third and fifth spectral components of the trajectory.

### 3.1.3. Non-linear dynamics features

This study considers an exploratory analysis of NLD features to model the handwriting dynamics of PD patients. This approach is motivated by the evidence reported in previous stud-

ies [13, 18]. Based on these reports, we believe that when the disease progresses, the handwriting becomes more distorted and chaotic. Thus, NLD features should be able to reveal specific characteristics in handwriting such that allow us to discriminate between PD patients and healthy controls. The NLD features considered in this study are extracted from the trajectory signal  $r(t)$  of the Archimedean spiral and from the sentence. To understand the NLD analysis, the concept of phase space should be introduced. It is a multidimensional representation that allows computing topological features of a chaotic system. For a time series  $s(n)$ , the phase space can be reconstructed using the embedding theorem introduced in [19]. The phase space is defined according to Equation 2, where  $\hat{s}(n)$  is the reconstructed attractor,  $n$  is the number of points in the time series, and  $m$  and  $\tau$  are the embedding dimension and time delay, respectively. The embedding dimension is estimated using the false neighbors method [20], and the time delay is found as the first minimum of the mutual information function.

$$\hat{s}(n) = \{s(n), s(n - \tau), \dots, s(n - (m + 1)\tau)\} \quad (2)$$

Figure 7 shows attractors corresponding to trajectories of the spirals introduced in Figure 6. Note that the PD patient exhibits

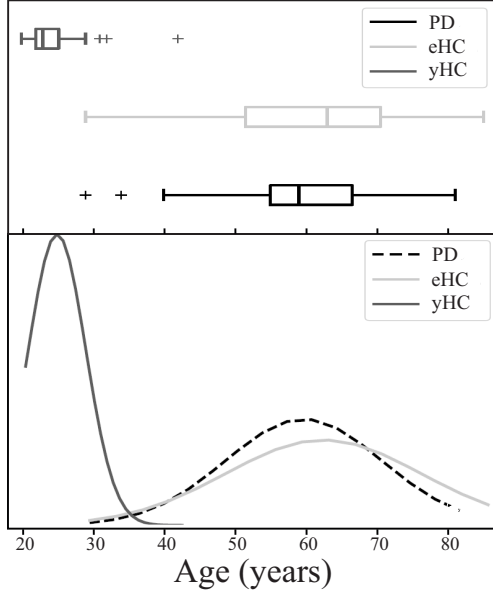


Figure 4: Age distribution of the three groups of subjects.

more irregular trajectories in its corresponding attractor than the HC subjects. Once the attractor is created, several features can be computed to measure its complexity. In this study a total of seven NLD features are extracted from the reconstructed attractors.

*Approximate entropy (ApEn):* The ApEn is a regularity statistic to measure the average conditional information generated by diverging points on trajectories in the attractor. A time series containing several repetitive patterns has a relatively small ApEn, while a more complex process has a higher ApEn. Details of the process to compute the ApEn are described in [21].

*Sample entropy (SampEn):* The main drawback of ApEn is its dependence on the signal's length due to self comparison of attractor's points. The SampEn is a modification of the ApEn which appears to overcome this drawback. Further details of the process to compute ApEn can be found in [22].

*Approximate and Sample entropies with Gaussian kernels:* The computation of ApEn and SampEn estimates the regularity of the attractor's trajectories by counting neighbor points. This process is performed using a Heaviside step function. Instead of using such a step function, the computation of ApEn and SampEn with Gaussian kernels uses the exponential function presented in Equation 3, where  $R$  is a tolerance parameter of the distance between near samples in the time-series  $s[n]$ . Further details of the computation process can be found in [23].

$$d_G(s[i], s[j]) = \exp\left(-\frac{\|s[i] - s[j]\|^2}{10R^2}\right) \quad (3)$$

*Correlation Dimension (CD):* This feature allows to estimate the exact space occupied by the attractor in the phase space. To estimate CD the correlation sum  $C(\varepsilon)$  is defined according to Equation 4, where  $\Theta$  is the Heaviside step function.  $C(\varepsilon)$  can be interpreted as the probability to have pairs of points in a trajectory of the attractor inside the same sphere of radius  $\varepsilon$ .

In [24], the authors demonstrated that  $C(\varepsilon)$  represents a volume measure, hence CD can be defined by Equation 5.

$$C(\varepsilon) = \lim_{n \rightarrow \infty} \frac{1}{n(n-1)} \sum_{i=1}^n \sum_{j=i+1}^n \Theta(\varepsilon - |s[i] - s[j]|) \quad (4)$$

$$CD = \lim_{\varepsilon \rightarrow 0} \frac{\log(C(\varepsilon))}{\log(\varepsilon)} \quad (5)$$

*Hurst exponent (HE):* This feature measures the long term dependence of a time series. It is defined according to the asymptotic behavior of the re-scaled range of a time series as a function of a time interval [25]. The estimation process consists of dividing the time series into intervals of size  $L$  and calculating the average ratio between the range  $R$  and the standard deviation  $\sigma$  of the time series. HE is computed as the slope of the curve obtained from Equation 6.

$$L^{HE} = \frac{R}{\sigma} \quad (6)$$

*Largest Lyapunov exponent (LLE):* This feature represents the average divergence rate of neighbor trajectories in the phase space. Its estimation process follows the algorithm in [26]. After the reconstruction of the phase space, the nearest neighbor of every point in the trajectory is estimated. The LLE is estimated as the average separation rate of those neighbors in the phase space.

*Lempel-Ziv complexity (LZC):* This feature measures the degree of disorder of spatio-temporal patterns in a time series [27]. In the computation process the signal is transformed into binary sequences according to the difference between consecutive samples, and the LZC reflects the rate of new patterns in the sequence. It ranges from 0 (deterministic sequence) to 1 (random sequence). Further details of the computation process can be found in [28, 29].

### 3.2. Classification

Three different classifiers are used in this study: (1) K-nearest neighbors, (2) SVM with a Gaussian kernel, and (3) random forest (RF). The three aforementioned classifiers were trained and tested following a leave one out cross-validation strategy. This procedure is repeated for each sample to assure that all data are tested. The parameters of the classifiers are optimized in a grid-search. For the KNN the possible number of neighbors was  $K \in \{3, 5, 7\}$ . For the SVM the parameters  $C$  and  $\gamma$  were optimized up to powers of ten where  $C \in \{0.0001, 0.001, \dots, 1000\}$  and  $\gamma \in \{0.0001, 0.001, \dots, 1000\}$ . Finally, for the RF the number of trees and their maximum depth were  $N \in \{5, 10, 15, 20, 50\}$  and  $D \in \{1, 2, 5, 10\}$ , respectively. The performance of the classifiers was evaluated considering several statistics including the F-score, accuracy, sensitivity, and specificity.

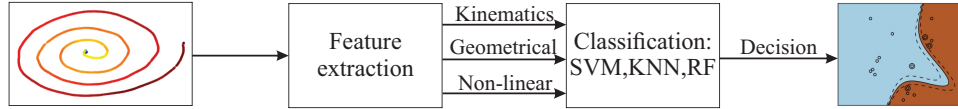


Figure 5: General methodology.

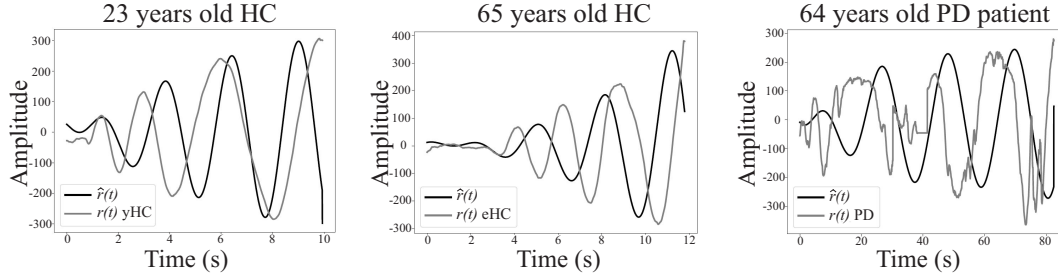


Figure 6: Comparison of the real trajectory of the Archimedean spiral  $r(t)$  and the model  $\hat{r}(t)$  for a yHC (left), an eHC (middle) and a PD patient (right).

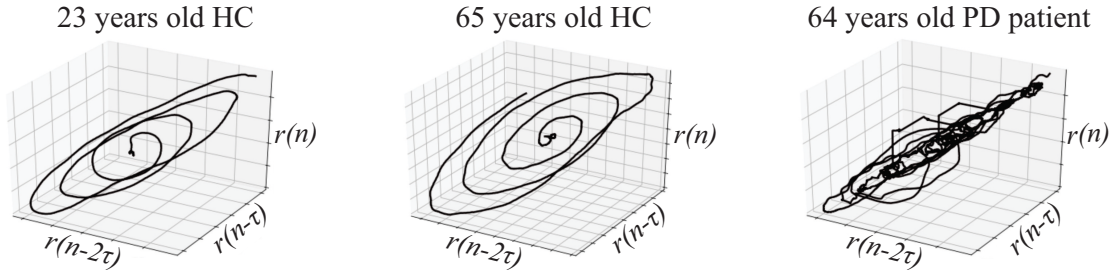


Figure 7: Attractors of the trajectory of the Archimedean spiral for a yHC (left), an eHC (middle) and a PD patient (right).

## 4. Experiments and results

A total of five experiments are performed in this study. Four of them comprise bi-class classification experiments: PD vs. yHC; PD vs. eHC; relevance analysis; and classification of PD vs. HC considering the separate validation sets described in Table 2. The fifth experiment is a multi-class classification task where the goal is to differentiate among four different stages of the disease. Details of all these experiments are described in the next subsections.

### 4.1. Classification of PD vs. yHC

Table 3 shows the results when PD patients vs. yHC subjects are classified using the aforementioned classifiers using different feature sets. We performed a Kruskal-Wallis test to assess whether a significant difference existed between the features computed from the PD patients and yHC subjects. The null hypothesis of both feature sets coming from the same distribution was rejected in all cases ( $p \ll 0.05$ ). The results obtained after the relevance analysis with PCA (see section 4.3) are also included in this table. The best results are obtained with the features computed from the Archimedean spiral ( $F1 = 0.94$ ). Note that in general the SVM and the RF classifiers provide the highest accuracies. Note also that there is a low variation of the optimal hyper-parameters along the feature sets and tasks,

which gives an idea about the stability and robustness of the proposed approach.

### 4.2. Classification of PD vs. eHC

The Kruskal-Wallis test to assess the significant difference between the features computed from the PD patients and eHC subjects reflect that both feature sets do not come from the same distribution ( $p \ll 0.05$ ). The results of the classification between PD patients and eHC subjects are shown in Table 4. This table also includes the results obtained after the relevance analysis with PCA (see section 4.3). Note that the results are slightly lower than those obtained in the discrimination of PD patients vs. yHC subjects. Although such a negative impact, high accuracies were also obtained when classifying PD patients vs. elderly HC subjects (F1 score of up to 0.87). The best results are obtained with the kinematic and kinematic + Geometrical feature sets. Similar to the previous case, the best classifiers in this experiment were the SVM and the RF. Note also that the dispersion of the hyper-parameters in this case is much larger than in the previous experiment, which gives count of the complexity of the classification problem. Note that the values of  $\gamma$  are, smaller than those in the previous experiment, indicating that the models are constrained and the set of support vectors should include a large number of training samples.

Figure 8 shows the Receiver Operating Characteristic (ROC) curves obtained from the previously described classification ex-

Table 3: Classification of PD patients vs. yHC subjects using SVM, KNN, and RF classifiers. **Kinem.**: kinematic features, **Geom.**: Geometrical features, **NLD**: NLD features, **Acc.**: Accuracy, **Spec.**: Specificity, **Sens.**: Sensitivity, **F1**: F1 score

Task	Feature set	SVM					KNN					RF						
		C	$\gamma$	Acc (%)	Spec	Sens	F1	K	Acc (%)	Spec	Sens	F1	N	D	Acc (%)	Spec	Sens	F1
Spiral	Kinem.	10	0.01	<b>94.0</b>	0.94	0.94	0.94	3	86.0	0.89	0.86	0.86	20	5	<b>92.4</b>	0.92	0.92	0.92
Spiral	Geom.	1	0.1	78.5	0.79	0.78	0.78	5	72.2	0.73	0.72	0.72	5	2	77.2	0.78	0.77	0.77
Spiral	Kinem.+Geom.	10	0.01	93.7	0.94	0.94	0.94	5	86.1	0.88	0.86	0.86	5	1	83.5	0.84	0.84	0.84
Spiral	NLD	1	0.1	77.2	0.77	0.77	0.77	5	69.6	0.71	0.70	0.69	5	1	67.1	0.67	0.67	0.67
Spiral	Kinem.+Geom.+NLD	10	0.01	91.1	0.91	0.91	0.91	5	87.3	0.90	0.87	0.87	15	1	88.6	0.89	0.89	0.89
Spiral	PCA Kinem.+Geom.+NLD	1	0.01	93.7	0.94	0.94	0.94	5	<b>88.6</b>	0.90	0.89	0.89	10	5	91.6	0.92	0.92	0.92
Sentence	Kinem.	1	0.01	92.0	0.92	0.92	0.92	3	86.7	0.88	0.87	0.86	50	5	90.7	0.91	0.91	0.91
Sentence	NLD	10	0.1	81.3	0.81	0.81	0.81	5	77.3	0.78	0.77	0.77	20	1	74.7	0.75	0.75	0.74
Sentence	Kinem.+NLD	10	0.001	93.3	0.93	0.93	0.93	3	85.3	0.86	0.85	0.85	50	5	89.3	0.89	0.89	0.89

Table 4: Classification of PD patients vs. eHC subjects using SVM, KNN, and RF classifiers. **Kinem.**: kinematic features, **Geom.**: Geometrical features, **NLD**: NLD features, **Acc.**: Accuracy, **Spec.**: Specificity, **Sens.**: Sensitivity, **F1**: F1 score

Task	Feature set	SVM					KNN					RF						
		C	$\gamma$	Acc (%)	Spec	Sens	F1	K	Acc (%)	Spec	Sens	F1	N	D	Acc (%)	Spec	Sens	F1
Spiral	Kinem.	100	0.001	87.0	0.87	0.87	0.87	3	<b>86.7</b>	0.87	0.86	0.86	10	1	<b>85.3</b>	0.85	0.85	0.85
Spiral	Geom.	100	0.0001	30.7	0.74	0.69	0.72	3	53.3	0.53	0.53	0.53	5	1	57.3	0.58	0.58	0.59
Spiral	Kinem.+Geom.	10	0.001	86.7	0.89	0.87	0.87	5	81.3	0.84	0.81	0.81	15	1	84.0	0.84	0.84	0.84
Spiral	NLD	0.0001	0.0001	52.0	0.73	0.52	0.64	7	58.7	0.59	0.59	0.59	5	1	56.0	0.58	0.56	0.58
Spiral	Kinem.+Geom.+NLD	100	0.0001	86.7	0.89	0.87	0.87	5	80.0	0.81	0.80	0.80	10	1	84.0	0.84	0.84	0.84
Spiral	PCA Kinem.+Geom.+NLD	10	0.001	<b>89.3</b>	0.89	0.89	0.89	3	81.3	0.81	0.81	0.81	50	5	81.0	0.81	0.81	0.81
Sentence	Kinem.	1	0.01	70.4	0.70	0.70	0.70	7	73.2	0.73	0.73	0.73	15	10	78.9	0.79	0.79	0.79
Sentence	NLD	100	0.01	62.0	0.62	0.62	0.62	5	63.4	0.63	0.63	0.63	50	1	60.6	0.61	0.61	0.61
Sentence	Kinem.+NLD	0.001	0.001	53.5	0.75	0.53	0.68	7	78.9	0.80	0.79	0.79	20	5	73.2	0.73	0.73	0.73

periments. These curves allow the comparison among results obtained in the classification of PD patients and the two groups of HC subjects. Only results from kinematic and geometrical features extracted from the Archimedean spiral are included. It can be observed that the three classifiers provide similar results in both experiments. The results when classifying PD vs. eHC confirm the negative impact of aging in the classification process. Histograms and the corresponding fitted probability den-

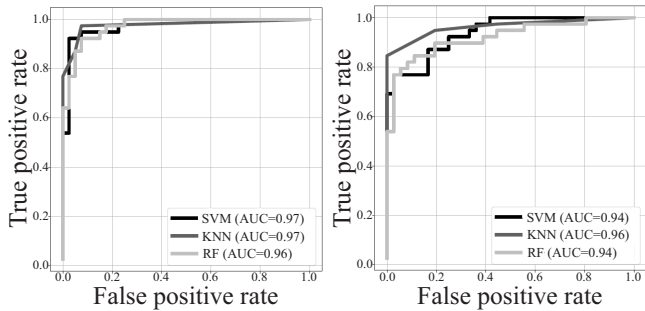


Figure 8: ROC curves for the classification of PD patients vs. young HC subjects (left) and for PD patients vs. elderly HC subjects (right).

sity distribution are shown in Figure 9. The figure illustrates the distribution of the SVM scores, i.e., the distance of data samples to the separating hyperplane. The statistical significance of the results was assessed with a Welch t-test to evaluate the difference in the scores obtained for PD patients and HC subjects. The null hypothesis was rejected for PD vs. yHC ( $t = -9.043$ ,  $p \ll 0.005$ ), and for PD vs. eHC ( $t = -12.817$ ,  $p \ll 0.005$ ).

#### 4.3. Relevance analysis

Apart from the typical classification between groups of subjects, we want to perform a relevance analysis such that al-

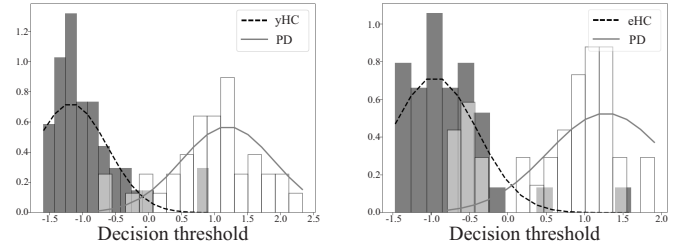


Figure 9: Histograms and the corresponding probability density distributions of the scores obtained from PD patients and yHC subjects (left), and for PD patients and eHC subjects (right).

lows the identification of the most relevant/discriminant features. This analysis help in finding features that could be potentially used in clinical practice not only to make informed decisions but to provide additional information to the clinician about the health state of a patient. In this paper the process is based on the Principal Component Analysis (PCA) algorithm. The original feature matrix  $X \in \mathbb{R}^{m \times p}$  is reduced to a matrix  $X_r \in \mathbb{R}^{m \times q}$ , ( $q < p$ ) according to a relevance vector  $\rho = [\rho_1, \rho_2, \dots, \rho_q, \dots, \rho_p]$  computed as  $\rho = \sum_{j=1}^p |\lambda_j \mathbf{v}_j|$ , where  $\lambda_j$  and  $\mathbf{v}_j$  are the eigenvalues and the eigenvectors of the original feature matrix [30]. The values of  $\rho$  for each feature are related with the contribution of the feature to each principal component. The original features with higher  $\rho$  are the most correlated with the principal components and are included to form the reduced feature space. This approach has been successfully used in previous studies and its main advantage over other existing feature selection methods is its low computational cost [31, 32]. In this work the relevance analysis is performed upon the feature space formed with kinematic, geometrical and NLD features extracted from the Archimedean spiral. 90% of the total

variance is kept in the reduced feature space which is formed with a total of 18 features for the case of PD vs. yHC, 19 features for PC vs. eHC, and 16 features for yHC vs. eHC. Table 5 indicates the top 10 of the selected features on each case.

Table 5: Top 10 of selected features from the Archimedean spiral.  $\Delta$  and  $\Delta\Delta$  indicate the first and second derivative, respectively.

PD vs. yHC	PD vs. eHC
Min. $\Delta\Delta$ pressure	$a_1$ of $\widehat{r}(t)$
Average speed	Skewness of acceleration
Average pressure	Kurtosis of acceleration
Kurtosis of speed	MSE between $r(t)$ and $\widehat{r}(t)$
Min. speed	Average acceleration
Skewness of $r(t)$	Std. of $\Delta z(t)$
Skewness of $\Delta\Delta$ pressure	2nd spectral component of $r(t)$
Max. speed	Max. acceleration
Min. $\Delta z(t)$	Min. acceleration
Std. of $\Delta z(t)$	LZC

The results indicate that the best features to classify PD patients and yHC subjects are those based on the kinematic analysis. When considering the case of PD patients vs. eHC, some of the geometrical and spectral features appear in the top ten of the selected features. Particularly, the first coefficient of the third-order polynomial ( $a_1$ ) used to model the amplitude of the trajectory  $\widehat{r}(t)$  appears in the first place of the top ten. Finally, note that the features selected in the case of eHC vs. yHC are mostly different compared to those selected in the previous cases.

The selected features were used to perform two classification experiments: PD vs. yHC and PD vs. eHC. Results are indicated in Tables 3 and 4, respectively. The aim is to evaluate the contribution of each selected feature in these classification tasks. Each feature was sequentially added according to the order given by the relevance factor  $\rho$ . The classification step is performed using a SVM. The results are shown in Figure 10A for PD vs. yHC, and in Figure 10B for PD vs. eHC. The bars indicate the relevance factor of each feature and the black lines indicate the obtained incremental accuracy. Note that when classifying PD vs. yHC about 90% of accuracy is obtained already with the first two relevant features, indicating that the problem is relatively simple and it can be solved with a low dimensional (less complex) feature space. Conversely, when classifying PD vs. eHC at least the first 16 features are required to reach accuracies of around 90%. This fact confirms the increased complexity of that problem due to the impact of aging in the handwriting process. We performed additional experiments (not reported here) using only those features that provide an incremental improvement in the accuracy, however, the results were not satisfactory, indicating that all of the selected features are relevant for the classification process.

#### 4.4. Classification using a separate validation set

This experiment is performed with the aim of evaluating the proposed approach in a more realistic scenario. Given that this set of additional subjects was recorded in sessions different than those of the other groups, it is possible to say that this additional

validation set represents a group of subjects who arrived in the clinics and performed a handwriting test to decide whether to continue with further screenings to validate their neurological condition. The results are shown in Table 6. Note that the parameters of the classifiers are the same as those used in Table 4, which means that no further optimization was performed over the system, i.e., the patients in the separated validation set never participated in the configuration/optimization of the classifiers. The accuracy obtained with the KNN and RF classifiers are above 83% in several cases with different feature sets extracted from the Archimedean spiral. These results are comparable to those obtained in the PD vs. eHC experiments, which confirms the generalization capability of the proposed approach when using the KNN and RF classifiers. The results with the SVM are not as high as with the other classifiers perhaps because the optimization of the two meta-parameters needs a fine tuning which was not performed in our experiments to avoid biased results due to over-fitting. Further experiments will be performed in the near future with data from more subjects in order to improve the stability and robustness of this classifier.

#### 4.5. Classification of PD patients in different stages of the disease

Four-class classification experiments were performed considering four groups: (1) HC subjects; (2) PD patients with MDS-UPDRS-III scores below 20 (initial stage-PD1); (3) PD patients with MDS-UPDRS-III scores between 20 and 40 (intermediate stage-PD2); and (4) PD patients with MDS-UPDRS-III scores above 40 (advance stage-PD3). Classification was performed with a multi-class SVM following a one vs. all strategy. Confusion matrices with the results are reported in Table 7. Results are presented in terms of accuracy (Acc), F1 score (F1), and the Cohen-Kappa index ( $\kappa$ ).

In this case only drawings of the Archimedean spiral were considered and only the feature sets that exhibited the best results in the experiments with the separate validation set were extracted: kinematic; kinematic + geometrical; and kinematic + geometrical + NLD (see Table 6). Additionally, we explored the suitability of the feature set selected with PCA which was previously used to classify between HC and eHC subjects (Section 4.3). The results indicate that HC subjects can be accurately classified, while the patients in advance stage (PD3) are the most difficult to be discriminated. The results with kinematic + geometrical features are similar to those obtained with kinematic + geometrical + NLD features, which likely indicates that the nonlinear features are not complimentary to the kinematic and geometrical ones, at least to discriminate different stages of PD. The confusion matrix also indicates that dimensionality reduction does not have positive impact in the results, conversely increases the false positive rate making the system to confuse HC subjects with patients in initial (PD1) or intermediate (PD2) stages of the disease.

## 5. Discussion

Kinematic features seem to be the most suitable to perform the automatic discrimination between PD patients and HC sub-

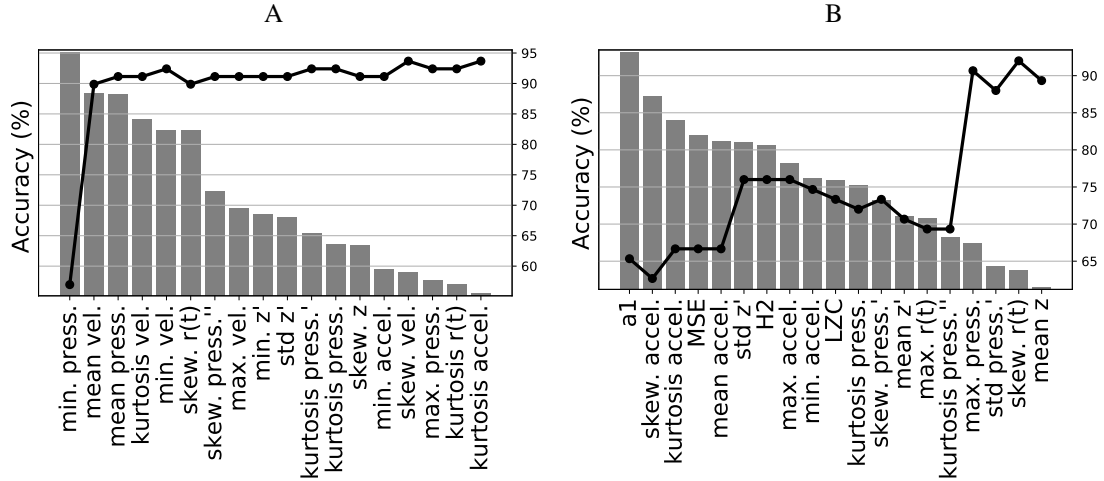


Figure 10: Classification of PD vs. yHC subjects (left) and PD vs. eHC subjects (right) when the selected features are sequentially added.

Table 6: Classification of PD patients vs. HC subjects using the separate validation set. **Kinem:** kinematic features, **Geom:** Geometrical features, **NLD:** NLD features, **Acc:** Accuracy, **Spec.** Specificity, **Sens.** Sensitivity, **F1:** F1 score

Task	Feature set	SVM						KNN				RF						
		C	$\gamma$	Acc (%)	Spec	Sens	F1	K	Acc (%)	Spec	Sens	F1	N	D	Acc (%)	Spec	Sens	F1
Spiral	Kinem.	100	0.001	50.0	0.50	0.50	0.50	3	<b>83.3</b>	0.83	0.83	0.83	10	1	66.6	0.69	0.66	0.66
Spiral	Geom.	100	0.0001	58.3	0.23	0.41	0.29	3	58.3	0.59	0.58	0.58	5	1	58.3	0.61	0.58	0.55
Spiral	Kinem.+Geom.	10	0.001	66.6	0.69	0.67	0.66	5	81.3	0.84	0.81	0.81	15	1	<b>83.3</b>	0.93	0.92	0.92
Spiral	NLD	0.0001	0.0001	50.0	0.75	0.50	0.66	7	58.4	0.59	0.58	0.59	5	1	64.3	0.65	0.65	0.65
Spiral	Kinem.+Geom.+NLD	100	0.0001	58.3	0.58	0.58	0.58	5	<b>83.3</b>	0.83	0.83	0.83	10	1	72.0	0.71	0.71	0.71
Spiral	PCA Kinem.+Geom.+NLD	10	0.001	66.6	0.66	0.66	0.66	3	66.6	0.66	0.66	0.66	50	5	50.0	0.50	0.50	0.52
Sentence	Kinem.	1	0.01	<b>75.0</b>	0.76	0.75	0.75	7	58.3	0.61	0.42	0.72	15	10	58.4	0.50	0.50	0.50
Sentence	NLD	100	0.01	58.3	0.59	0.59	0.59	5	59.0	0.59	0.59	0.61	50	1	51.2	0.51	0.51	0.51
Sentence	Kinem.+NLD	0.001	0.001	50.0	0.75	0.50	0.66	7	50.0	0.50	0.50	0.67	20	5	51.3	0.51	0.51	0.51

Table 7: Confusion matrices with results of classifying HC subjects and PD patients in different stages of the disease. PD1: patients with MDS-UPDRS-III scores between 0 and 20. PD2: patients with MDS-UPDRS-III scores between 21 and 40. PD3: patients with MDS-UPDRS-III scores above 40. Spiral PCA indicates the results obtained with the set of 19 features that results after the feature selection process when classifying PD vs. eHC (see Figure 10). The results are expressed in (%). F1: F1 score.  $\kappa$ : Cohen-kappa index.

	Spiral Kinem.				Spiral Kinem.+Geom.				Spiral Kinem+Geom+NLD				Spiral PCA			
	Acc=61.3, F1=0.58, $\kappa$ =0.40				Acc=64.0, F1=0.62, $\kappa$ =0.44				Acc=64.0, F1=0.62, $\kappa$ =0.44				Acc=57.3, F1=0.55, $\kappa$ =0.36			
	HC	PD1	PD2	PD3												
HC	97.2	0.0	2.8	0.0	97.2	0.0	2.8	0.0	97.2	0.0	2.8	0.0	91.7	2.8	5.5	0.0
PD1	15.4	30.8	15.4	38.5	15.4	38.5	7.7	38.5	15.4	38.5	15.4	30.8	15.4	38.5	15.4	30.8
PD2	21.4	28.6	35.7	14.3	21.4	14.3	28.6	35.7	21.4	21.4	28.6	28.6	28.6	28.6	28.6	14.3
PD3	33.3	33.3	16.7	16.7	33.3	16.7	16.7	33.3	33.3	16.7	16.7	33.3	0.0	50.0	41.7	8.3

jects (young or elderly). The combination of the three feature sets in the same space also exhibited good classification results. Besides the binary classification, a relevance analysis was performed. According to the results, the most discriminative features are geometrical and kinematic. Most of the selected features as relevant are related to speed, pressure, and acceleration of the strokes, which is related to the deficits exhibited by patients when performing motor activities like handwriting. Patients in different stages of the disease were also classified and  $\kappa$  indexes between 0.36 and 0.44 were obtained. The results indicate that, at least in the experiments performed here, the nonlinear features do not contribute to improve the classification of different stages of the disease. An additional experiment with a separate validation set with PD and HC subjects was performed. This validation set was built during recording sessions

different than those performed to collect the signals considered in the other experiments. Thus this additional experiment allows the evaluation of the proposed approach in real conditions. The results show that it is possible to discriminate between PD and HC subjects (in the separate validation set) with accuracies of up to 83.3%. To the best of our knowledge, this is the first work that considers experiments with separate and independent validation samples. Further research should be performed by combining the proposed model with novel approaches based on deep learning methods [16, 14]. In addition, longitudinal studies should be performed to understand and track the progress of the disease in the PD patients through time.

## 6. Conclusion

This paper explored and evaluated the suitability of three different feature sets (kinematic, geometrical and NLD) to model handwriting impairments exhibited by PD patients. We provide an accurate method to classify between Parkinson's patients and healthy subjects. The model was validated in a different dataset, and high accuracies were obtained (83.3%). The classification of Parkinson's patients in several stages of the disease is promising. We are aware of the fact that more research and a larger sample of patients is necessary to lead to more conclusive results; however, we think that the results presented here are a step forward to the development of non-intrusive methods, useful in clinical practice, to diagnose and monitor Parkinson's patients.

Future studies will include the comparison of the proposed approach with recent studies based on deep learning strategies, which have shown to be also accurate to model the handwriting deficits of PD patients.

## Acknowledgments

The authors thank to the patients of Fundalianza Parkinson Colombia for their invaluable support of this study. This work was financed by CODI from UdeA grants PRG2015-7683 and PRV16-2-01, and from the European Unions Horizon 2020 research and innovation programme under the Marie Skłodowska-Curie Grant Agreement No. 766287.

*Ethical Approval and informed consent:* Informed consent was obtained from all participants of the study. All procedures were in accordance with the ethical standards of the institutional research committee and with the 1964 Helsinki declaration and its later amendments. The procedures were approved by the Ethical Research Committee of the University of Antioquia.

## References

### References

- [1] O. Hornykiewicz, Biochemical aspects of Parkinson's disease, *Neurology* 51 (2 Suppl 2) (1998) S2-S9.
- [2] R. F. Pfeiffer, Z. K. Wszolek, Parkinson's disease, CRC Press, 2004.
- [3] A. Letanneux, J. Danna, J. Velay, F. Viallet, S. Pinto, From micrographia to parkinson's disease dysgraphia, *Movement Disorders* 29 (12) (2014) 1467-1475.
- [4] C. G. Goetz, et al., Movement Disorder Society-sponsored revision of the Unified Parkinson's Disease Rating Scale (MDS-UPDRS): Scale presentation and clinimetric testing results, *Movement Disorders* 23 (15) (2008) 2129-2170.
- [5] R. Pahwa, K. E. Lyons, Handbook of Parkinson's disease, CRC Press, 2013.
- [6] A. Schrag, Y. B. Ben-Shlomo, N. Quinn, How valid is the clinical diagnosis of Parkinson's disease in the community?, *Journal of Neurology, Neurosurgery & Psychiatry* 73 (5) (2002) 529-534.
- [7] S. J. Johnson, M. D. Diener, A. Kaltenboeck, H. G. Birnbaum, A. D. Siderowf, An economic model of Parkinson's disease: implications for slowing progression in the United States, *Movement Disorders* 28 (3) (2013) 319-326.
- [8] Y. Sarbaz, F. Towhidkhalah, V. Mosavari, A. Janani, A. Soltanzadeh, Separating parkinsonian patients from normal persons using handwriting features, *Journal of Mechanics in Medicine and Biology* 13 (03) (2013) 1350030.
- [9] S. Rosenblum, M. Samuel, S. Zlotnik, I. Erikh, I. Schlesinger, Handwriting as an objective tool for Parkinson's disease diagnosis, *Journal of Neurology* 260 (9) (2013) 2357-2361.
- [10] P. Drotár, J. Mekyska, I. Rektorová, L. Masarová, Z. Smékal, M. Faundez-Zanuy, Evaluation of handwriting kinematics and pressure for differential diagnosis of parkinson's disease, *Computer Methods and Programs in Biomedicine* 117 (3) (2014) 405-411.
- [11] P. Drotár, J. Mekyska, I. Rektorová, L. Masarová, Z. Smékal, M. Faundez-Zanuy, Evaluation of handwriting kinematics and pressure for differential diagnosis of Parkinson's disease, *Artificial intelligence in Medicine* 67 (2016) 39-46.
- [12] J. C. Vásquez-Correa, J. R. Orozco-Arroyave, et al., Multi-view representation learning via GCCA for multimodal analysis of Parkinson's disease, in: 42nd IEEE International Conference on Acoustics, Speech, and Signal Processing (ICASSP), 2017, pp. 2966-2970.
- [13] K. López-de Ipiña, A. Bergareche, P. De La Riva, M. Faundez-Zanuy, P. M. Calvo, J. Roure, E. Sesa-Nogueras, Automatic non-linear analysis of non-invasive writing signals, applied to essential tremor, *Journal of Applied Logic* 16 (2016) 50-59.
- [14] C. R. Pereira, D. R. Pereira, G. H. Rosa, V. H. Albuquerque, S. A. Weber, C. Hook, J. Papa, Handwritten dynamics assessment through convolutional neural networks: An application to parkinson's disease identification, *Artificial intelligence in medicine* 87 (2018) 67-77.
- [15] C. Gallicchio, A. Micheli, L. Pedrelli, Deep echo state networks for diagnosis of parkinson's disease, arXiv preprint arXiv:1802.06708.
- [16] J. C. Vasquez-Correa, T. Arias-Vergara, J. R. Orozco-Arroyave, B. Eskofier, J. Klucken, E. Nöth, Multimodal assessment of parkinson's disease: a deep learning approach, *IEEE journal of biomedical and health informatics* (In press).
- [17] C. De Boor, A practical guide to splines, Vol. 27, Springer-Verlag New York, 1978.
- [18] M. G. Longstaff, R. A. Heath, A nonlinear analysis of the temporal characteristics of handwriting, *Human Movement Science* 18 (4) (1999) 485-524.
- [19] F. Takens, et al., Detecting strange attractors in turbulence, *Lecture notes in mathematics* 898 (1) (1981) 366-381.
- [20] M. B. Kennel, R. Brown, H. D. Abarbanel, Determining embedding dimension for phase-space reconstruction using a geometrical construction, *Physical review A* 45 (6) (1992) 3403.
- [21] S. Pincus, Approximate entropy (ApEn) as a complexity measure, *Chaos: An Interdisciplinary Journal of Nonlinear Science* 5 (1) (1995) 110-117.
- [22] J. S. Richman, J. R. Moorman, Physiological time-series analysis using approximate entropy and sample entropy, *American Journal of Physiology-Heart and Circulatory Physiology* 278 (6) (2000) H2039-H2049.
- [23] L. S. Xu, K. Q. Wang, L. Wang, Gaussian kernel approximate entropy algorithm for analyzing irregularity of time-series, in: *International Conference on Machine Learning and Cybernetics*, Vol. 9, 2005, pp. 5605-5608.
- [24] P. Grassberger, I. Procaccia, Measuring the strangeness of strange attractors, in: *The Theory of Chaotic Attractors*, Springer, 2004, pp. 170-189.
- [25] H. E. Hurst, Long term storage: An experimental study, Constable, London, 1965.
- [26] M. T. Rosenstein, J. J. Collins, C. J. De Luca, A practical method for calculating largest lyapunov exponents from small data sets, *Physica D: Nonlinear Phenomena* 65 (1-2) (1993) 117-134.
- [27] A. Lempel, J. Ziv, On the complexity of finite sequences, *IEEE Transactions on information theory* 22 (1) (1976) 75-81.
- [28] F. Kaspar, H. G. Schuster, Easily calculable measure for the complexity of spatiotemporal patterns, *Physical review A* 36 (2) (1987) 842-848.
- [29] C. Travieso, J. Alonso, J. R. Orozco-Arroyave, J. Vargas-Bonilla, E. Nöth, R.-G. A.G., Detection of different voice diseases based on the nonlinear characterization of speech signals, *Expert Systems With Applications* (82) (2017) 184-195.
- [30] G. Daza-Santacoloma, J. D. Arias-Londoño, J. I. Godino-Llorente, N. Sáenz-Lechón, V. Osma-Ruiz, G. Castellanos-Domínguez, Dynamic feature extraction: an application to voice pathology detection, *Intelligent Automation & Soft Computing* 15 (4) (2009) 667-682.

- [31] J. R. Orozco-Arroyave, S. Murillo-Rendón, et al., Automatic selection of acoustic and non-linear dynamic features in voice signals for hypernasality detection, in: 12th International Conference of the Speech Communication Association (INTERSPEECH), 2011, pp. 529–532.
- [32] T. Arias-Vergara, J. C. Vásquez-Correa, J. R. Orozco-Arroyave, Parkinson's Disease and Aging: Analysis of Their Effect in Phonation and Articulation of Speech, *Cognitive Computation* 9 (6) (2017) 731–748.